ISPRS Journal of Photogrammetry and Remote Sensing 208 (2024) 233–244

Contents lists available at ScienceDirect

ISPRS Journal of Photogrammetry and Remote Sensing

journal homepage: www.elsevier.com/locate/isprsjprs

Revealing the spatial variation in biomass uptake rates of Brazil's secondary forests

Na Chen [a,*], Nandin-Erdene Tsendbazar [a], Daniela Requena Suarez [a], Celso H.L. Silva-Junior [b,c,d], Jan Verbesselt [a], Martin Herold [a,e]

[a] Laboratory of Geo-information Science and Remote Sensing, Wageningen University & Research, Droevendaalsesteeg 3, 6708 PB Wageningen, the Netherlands
[b] Instituto de Pesquisas Ambientais da Amazônia, Brasília, DF, Brazil
[c] Department of Geography, School of Environment Education and Development, The University of Manchester, Oxford Road, Manchester M13 9PL, UK
[d] Programa de Pós-graduação em Biodiversidade e Conservação, Universidade Federal do Maranhão - UFMA, São Luís, MA, Brazil
[e] Helmholtz GFZ German Research Centre for Geosciences, Section 1.4 Remote Sensing and Geoinformatics, Telegrafenberg, Potsdam 14473, Germany

ARTICLE INFO

Keywords:
AGB recovery
Forest age
GWR
Remote sensing
Secondary forests
Surrounding tree cover

ABSTRACT

Monitoring forest aboveground biomass (AGB) is essential for quantifying the carbon cycle and mitigating climate change. Tropical secondary forests are significant carbon sinks that sequester large amounts of carbon dioxide. While recent studies have attempted to estimate the AGB recovery rates in tropical forests, considerable uncertainty remains in the estimation of AGB recovery of secondary forests and the spatial variability of the effects that different environmental conditions and degrees of human use may have on AGB recovery. These knowledge gaps hinder further understanding of climate change mitigation potential of secondary forests. Remote sensing products provide spatially and temporally explicit information for understanding and monitoring secondary forest dynamics. To explore the local effects of different factors on AGB of secondary forests in Brazil, we used geographically weighted regression (GWR) models that account for spatial heterogeneity in geospatial data to estimate the AGB of secondary forests in Brazil. Secondary forest areas (29142 polygons) were extracted from Brazil's forest age maps between 1984 and 2019. The AGB of these areas was derived from the Climate Change Initiative Biomass maps. The effects of selected predictors such as forest age, climatic water deficit, the cation exchange capacity of soil and surrounding tree cover were analyzed. The two most influential factors, forest age and surrounding tree cover were utilized to estimate the AGB and the recovery rates per year. Our results show the high spatial variation of different predictors' effects on the AGB of secondary forests. Also, the GWR model (with an adjusted R^2 of 0.74) showed considerable improvements regarding "goodness of fit" of models compared with the Ordinary Least Squares (with an adjusted R^2 of 0.53). Our estimated average AGB recovery rate across all Brazil's biomes is 7.5 Mg ha^{-1} yr^{-1} (using forest age) for the first 20 years. We presented the map of the spatial variation of AGB recovery rates in Brazil. The estimated AGB recovery rates range using forest age is 28.9 Mg ha^{-1} yr^{-1}. Our estimated mean AGB recovery rates of different biomes are 17.7 % on average higher than IPCC default rates. Our results provide baseline information for reducing uncertainties related to carbon sink estimation of secondary forests in Brazil, hence assisting in developing sustainable forest management and ecosystem restoration strategies.

1. Introduction

Secondary forests are playing increasingly important roles in the global carbon cycle. Secondary forests are forests that regrow in regions that have experienced complete forest removal (Chokkalingam & De Jong, 2001). The secondary forests increased rapidly in their extent and covered more than 60 % of the global forest at the end of the 20th century (Orihuela-Belmonte et al., 2013; Mackey et al., 2015; Pain et al., 2021). A previous study estimated the aboveground biomass (AGB) recovery rate of young secondary forests in the Neotropics and found that the carbon uptake rate is eleven times of that in old-growth forests (Poorter et al., 2016). Research carried out in the secondary forests of the Amazon biome revealed that the mean gross carbon sequestration increased substantially from 1986 (10.38 ± 9.7 million Mg) to 2017

* Corresponding author.
E-mail address: na.chen@wur.nl (N. Chen).

https://doi.org/10.1016/j.isprsjprs.2023.12.013
Received 29 June 2023; Received in revised form 29 November 2023; Accepted 18 December 2023
Available online 25 January 2024

(66.12 ± 9.7 million Mg CO_2) (Smith et al., 2020).

Evaluating why and where the AGB recovery of secondary forest varies is essential for the quantifying potential of secondary forest. Many factors, such as forest age, climate, terrain, soil, water availability, landscape, disturbance and land use history affect AGB recovery in secondary forests (César et al., 2021; Cook-Patton et al., 2020; Crk et al., 2009; Becknell et al., 2018; Heinrich et al., 2021, 2023; Poorter et al., 2016; Pugh et al., 2019; Requena Suarez et al., 2021,2023; Sundqvist et al., 2013). Previous researchers have attempted to evaluate the effects of different factors on the AGB regrowth of secondary forests. For example, Poorter et al. (2016) evaluated the effects of climate, soil fertility, forest cover, and previous land use on biomass resilience and has revealed that biomass resilience is driven by climatic water deficit. Becknell and Powers (2014) examined the effect of age, functional traits and soils on the AGB and found that the AGB increases with forest age in a secondary tropical dry forest, age alone could explain approximately half of the variation in AGB plots. Chen et al. (2023) assessed how secondary forest AGB is affected by different environmental and human factors using geospatial data and found that AGB recovery was mainly influenced by time since disturbance. Similar research also assessed the effects of different drivers (e.g. forest age, surrounding tree cover, soil characteristics) on the recovery of AGB in a tropical secondary forest of Costa Rica and results show that soil fertility has no significant effect on the AGB, AGB is positively related to age and surrounding tree cover, defined as the percentage of forest cover within a one-kilometer radius surrounding each plot (STC) (Oberleitner et al., 2021). Despite the increased interest in estimating the AGB recovery rates and how different factors affect these rates. AGB and its recovery have large variations in space. For example, the AGB recovery after 20 years has an eleven-fold variation across different sites in Neotropics (Poorter et al., 2016). The variation is even larger at a global scale, where a 100-fold variation of aboveground carbon accumulation rates in natural forest regrowth was observed (Cook-Patton et al., 2020). Previous studies have assessed the AGB recovery in Neotropics or Amazon biome (Heinrich et al., 2021; Poorter et al., 2016). However, spatially explicit information on how AGB recovery rates and its influencing factors vary in space in Brazil on a country scale is lacking.

Remote sensing data provides key opportunities for assessing the influence of different factors on the AGB in space, given that it provides spatially and temporally explicit information and has been widely used for forest monitoring. For example, optical images (e.g. Landsat images) have been commonly used to derive spectral information to monitor forest recovery (de Keersmaecker et al., 2022; DeVries et al., 2015; Decuyper et al., 2022; White et al., 2022). Optical imagery, Synthetic Aperture Radar and LiDAR data alone or in combination have been used to estimate forest AGB (Ahmed et al., 2013; David et al., 2022; Urbazaev et al., 2018). Based on satellite images, forest age, AGB, and tree cover maps and other remote sensing derived products at a regional or global scale have become feasible (Buchhorn et al., 2020; Santoro et al., 2021; Silva Junior et al., 2020).

Various spatial models can be used to capture the spatially varying relationships between variables. Geographically Weighted Regression (GWR) is a powerful spatial technique that takes spatial heterogeneity into consideration (Fotheringham et al., 2002). GWR models have been extensively used in many domains, such as environment (Pasculli et al., 2014; Tian et al., 2012), ecology (Kang et al., 2014; Wang et al., 2005), meteorology and climatology (Chao et al., 2018; Wang et al., 2012) economics (Jin et al., 2019; Lu et al., 2011), transportation (Cardozo et al., 2012; Dziauddin et al., 2015), health (Ge et al., 2017; Wang et al., 2010; Xu et al., 2022). GWR is able to analyze spatially varying relationships as well as provide local regression coefficients (Ge et al., 2017; Lu et al., 2022). Therefore, the capability of providing location-wise parameters for each variable makes GWR suitable and attractive for analyzing the effects of different factors on AGB locally.

Here, we aim to evaluate the local effects of different factors on regrowing forests of Brazil using geospatial data. Factors derived from remote sensing data, including forest age, elevation, slope, climatic water deficit (CWD), soil cation exchange capacity (CEC), soil total Nitrogen, STC, fire frequency, distance to settlements, and distance to roads were selected for further analysis. We further focused on factors that can be directly monitored using remote sensing data. Specifically, we aim to (1) assess the local effects of the aforementioned spatial factors on the secondary forest AGB in Brazil, (2) analyze the spatially varying effects of forest age on secondary forest AGB and (3) estimate the AGB recovery rates of secondary forests in Brazil.

2. Materials and methods

2.1. Study area

Brazil covers more than 8.5 million km^2, with forests covering 59 % of its total area and it is the second-largest forested area in the world (Shimabukuro et al., 2020). Brazil can be divided into six biomes, the Amazon, Atlantic Forest, Caatinga, Cerrado, Pampa and Pantanal (Fig. 1b) (Souza et al., 2020). The Amazon forest is the largest continuous tropical forest on earth (Silva Junior et al., 2022). Cerrado is the largest savanna in South America (De Castro et al., 2016). The Caatinga biome is located in the northeast of Brazil and the predominant land cover in the Caatinga biome is non-forest natural vegetated areas. The main forest types in Atlantic Forest are tropical moist forests and tropical seasonal forests. Historically, the Atlantic Forest biome suffered a tremendous loss of the original Atlantic forests (Ribeiro et al., 2009). Pampa is dominated by grasslands, sparse shrubs, and tree formation (Roesch et al., 2009). Pantanal is the largest tropical wetland on Earth (Ivory et al., 2019). Based on CCI Biomass (Supplementary material Table 1), the average AGB of biome Amazon is the largest (185.7 Mg ha^{-1}), followed by Atlantic Forest (113.2 Mg ha^{-1}), Pantanal (94.3 Mg ha^{-1}), Cerrado (83.4 Mg ha^{-1}), Pampa (75.0 Mg ha^{-1}), and Caatinga (36.1 Mg ha^{-1}). Based on the precipitation data of "TerraClimate" in 2019 (Abatzoglou et al., 2017), the Amazon has the greatest annual precipitation (2464 mm), followed by Pampa (1464 mm), Atlantic Forest (1142 mm), Cerrado (1033 mm), Pantanal (808 mm) and Caatinga (594 mm).

2.2. Extraction of explanatory variables from the geospatial dataset

Forest age maps of Brazil from 1984 to 2019 (Silva Junior et al., 2020) were utilized to extract the forest age for secondary forests. The edge pixels (pixels at the boundary or transition between secondary forests and non-secondary forests in an image) of the forest age raster layers from 1984 to 2019 were removed. Next, the raster age layers were converted to polygons and polygons that were smaller than 1 ha were excluded for further analysis. This was done to match the scale of the global AGB map (with a spatial resolution of 100 m). Tree cover was derived from "Copernicus Global Land Cover" maps (Buchhorn et al., 2020, Fig. 2). The "Copernicus Global Land Cover" maps were derived from the PROBA-V 100 m time-series data (Buchhorn et al., 2020).

Elevation and slope were chosen to examine the effect of topography on the AGB of secondary forests. Elevation data was derived from the Digital Elevation Models (DEM) from the "Shuttle Radar Topography Mission" (Farr et al., 2007), and was utilized to compute slope (in degrees). To assess the water availability's effect on AGB, the Climatic water deficit (CWD) in 2019 was averaged over all the monthly "def" layers of the "TerraClimate" global dataset (Abatzoglou et al., 2017, Fig. 2). To evaluate the effects of soil fertility on AGB, we derived the soil total Nitrogen and the soil CEC from the 'Soil Grids 250 m v2.0' product (Poggio et al., 2021, Fig. 2). SoilGrids provides global soil attributes maps by utilizing approximately 240,000 soil observations, more than 400 environmental variables and machine learning approaches to predict soil attributes (Poggio et al., 2021). To assess the influence of STC, the area of stable forest (in ha) within 500 m distance of the centroid of each secondary forest patch were calculated. Stable forest layers were

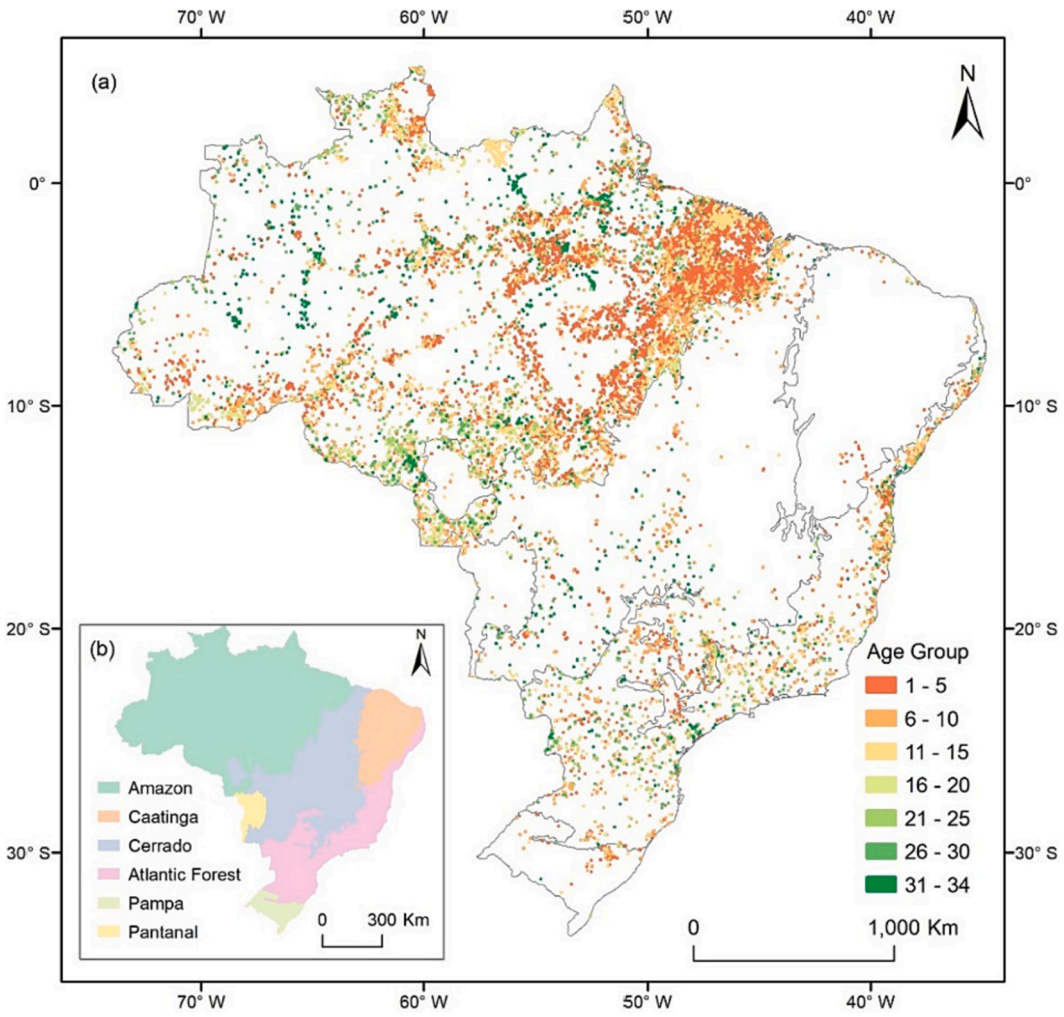

Fig. 1. Study area and distribution of secondary forests in different forest age groups of Brazil.

overlayed from the yearly forest map 1985–2019 derived from LUCC maps provided by the MapBiomas Project (MapBiomas Collection 6). Before overlaying the yearly forest maps, surface water was masked using the max water surface extent data from Joint Research Centre (Pekel et al., 2016) for accounting commission errors of forest maps. The sum of fire frequency from 1985 to 2019 was derived from the MapBiomas project (Mapbiomas Fire-Collection1; https://mapbiomas.org/en/colecoes-mapbiomas-1). To evaluate the effect of human use, we used distance to roads and settlements as proxies. The distance of the secondary forest to the closest roads and settlements was calculated using the 'Near' function of ArcGIS 10.6.1 based on the roads and settlements data acquired from OpenStreetMap (OpenStreetMap Contributors, 2021).

Before extracting the values of the explanatory variables, the geospatial data was reprojected to the same coordinate system (WGS84). After that, all the explanatory variables (except forest age, and fire) were resampled to 100 m spatial resolution to minimize the error caused by scale mismatch of datasets, and the mean value within each polygon was extracted in GEE. Resampling was not applied to forest age and fire frequency because the forest age has already been extracted as an attribute of polygons while converting from the raster layer and fire frequency maps were not resampled to keep their original values. Table 1 presents the statistical information of the chosen variables.

2.3. Extraction of aboveground biomass of secondary forests

The global AGB maps in 2018 (with 100 m spatial resolution) from Climate Change Initiative (CCI) Biomass project (Santoro et al., 2021) were downloaded, subsetted to the extent of Brazil and then uploaded to the GEE platform. Next, the mean AGB of each secondary forest polygon was calculated from the global CCI Biomass map. The descriptive statistics of the AGB for different biome were present in Supplementary material Table 1. We adopted the CCI AGB map because it is suitable for analysing biomass accumulation in secondary tropical forests and it was generated from radar data, less susceptible to saturation for high biomass values (Heinrich et al., 2021, 2023). However, a previous study has revealed that the CCI biomass map tends to overestimate low AGB and underestimate high AGB (Araza, et al., 2022). Other global or regional AGB maps, such as global biomass map produced by JPL (Saatchi et al., 2011) and biomass map based on LiDAR data collected by the "improving biomass estimation methods for the Amazon" (EBA) project (Ometto et al., 2023), also could be investigated in future studies.

2.4. Data analysis

After extracting the values of input variables to the secondary forest polygons (Table 1), polygons with AGB equal to 0 were removed and 29,142 polygons remained for further analysis. Natural log transformation was applied to the forest age variable to consider the non-

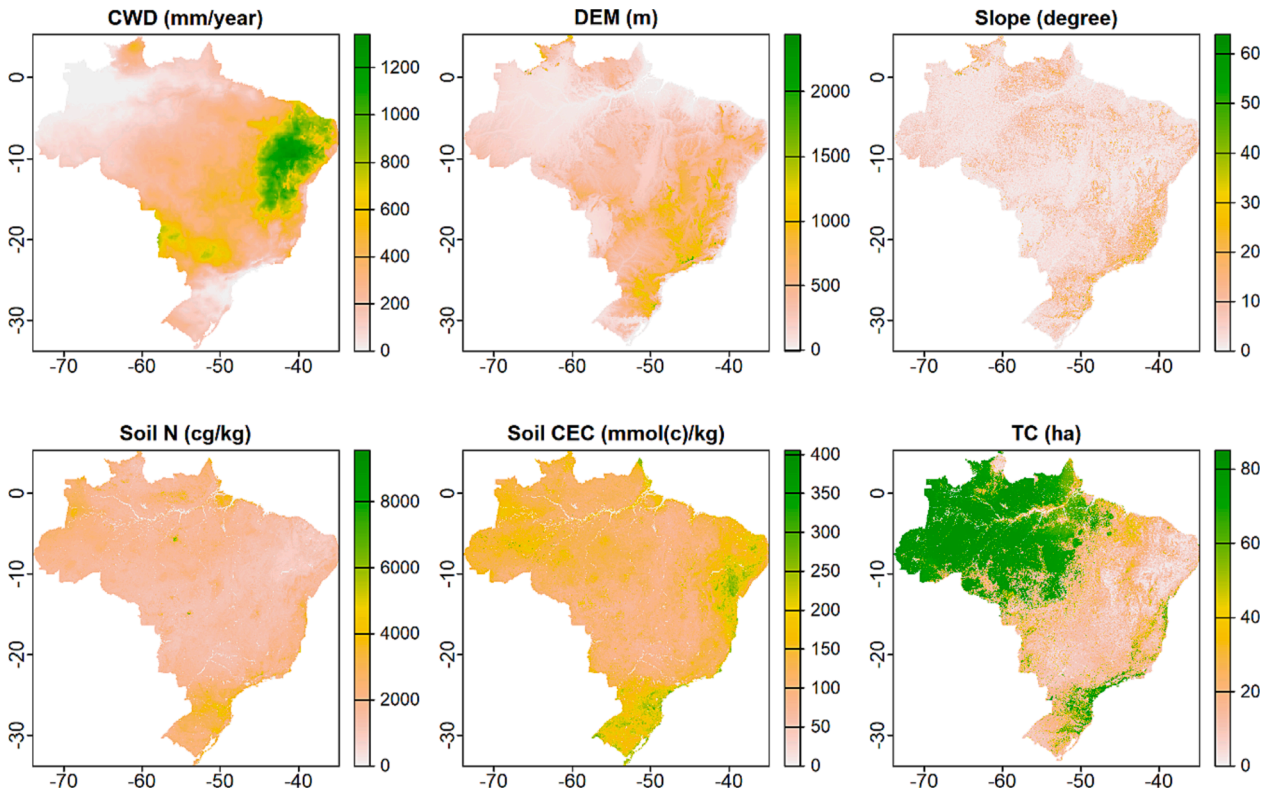

Fig. 2. Spatial distribution of continuous remote sensing variables for the GWR model.

Table 1
Descriptive statistics of environmental and human use variables.

Variable	Unit	Range	Mean	SD	Spatial resolution	Time	Source
Aboveground biomass (AGB)	Mg ha^{-1}	0 – 552.8	172.1	107.1	100 m	2018	(Santoro et al., 2021)
Tree cover	%	0 –100.0	83.7	19.0	100 m	2019	(Buchhorn et al., (2020)
Forest age	year	1 – 34.0	10.9	10.0	30 m	2019	(Silva Junior et al., 2020)
Elevation	meter	0.9 – 1905.5	221.7	196.2	30 m	2000	SRTM
Slope	degree	0.8 – 49.4	5.4	4.9	30 m	2000	Calculated
Climatic water deficit (CWD)	mm/year	0 – 855.5	237.0	113.6	4638 m	2019	(Abatzoglou et al., 2017)
Soil cation exchange capacity	mmol(c)/kg	0 – 313.3	112.2	31.8	250 m	/	(Poggio et al., 2021)
Soil total N (0–30 cm mean)	cg/kg	0 – 7427.0	1806.0	460.3	250 m	/	(Poggio et al., 2021)
Surrounding tree cover (STC)	ha	0 – 77.1	32.2	25.2	/	2019	Calculated from Mapbiomas
Distance to settlements	km	0.1 – 400.0	24.2	33.3	/	2021	OpenStreetMap contributors (2021)
Distance to roads	km	0 – 379.0	19.2	36.7	/	2021	OpenStreetMap contributors (2021)
Fire frequency (1985–2019)	times	0 – 19.0	0.8	1.5	30 m	1985– 2019	Mapbiomas (Alencar et al., 2022)

linear relationship between AGB and time. All variables were subtracted by mean and then divided by standard deviations using the "scale", a built-in function in R. A correlation coefficient between predictors was calculated and a correlation coefficient larger than 0.7 or less than −0.7 indicate strong linear relationships (Ratner, 2009). The correlation between distance to settlements and distance to roads was 0.79, hence the distance to settlement was excluded from further analysis.

2.4.1. Ordinary Least Squares regression

Traditionally, the OLS model is widely used for estimating forest AGB (Li et al., 2019; Lu, 2006). The OLS was selected for estimating the forest AGB and it serves as a base model to examine the global relationship between variables. OLS was fitted as:

$$Y = \beta_0 + \beta_1 X_1 + \beta_2 X_2 + \cdots + \beta_k X_k + \varepsilon \quad (1)$$

where Y is the dependent variable, β_0 is the intercept, β_k (k = 1, …,10) are estimated coefficients and ε denotes random error. R^2, Adjusted R^2 (corrected goodness-of-fit) and AICc (Corrected Akaike information criterion) were computed to evaluate the OLS Regression models.

2.4.2. Geographically weighted regression (GWR)

GWR is a local linear model that enables regression coefficients to vary in space by providing local-specific estimated parameters for each regression model (Fotheringham et al., 2002). The GWR model was selected to map the spatial variation of selected factors' effects on AGB of secondary forests. A GWR model was fitted as (Fotheringham, Brunsdon,and Charlton, 2002):

$$y_i = \beta_0(\mu_i, v_i) + \sum_{j=1}^{n} \beta_j(\mu_i, v_i) x_{ij} + \varepsilon_i \quad (2)$$

where y_i is the dependent variable of location i, $\beta_0(\mu_i, v_i)$ denote the local intercept, β_j are the estimated coefficients, n represents the number of independent variables, (μ_i, v_i) are the coordinates of the locations, x_{ij} are k th independent variable and ε_i is the random error at location i (Brunsdon et al., 1996; Lu et al., 2022). Adjusted R^2 and AICc were computed to evaluate the performance of models. According to Tobler's first law of geography, nearby things are more similar than those that are farther apart (Tobler, 1970). In line with the first law, GWR consists of local regressions that consider the nearby locations and different

weights are assigned to the neighbours based on the distance-decay kernel function (Lu et al., 2014). Several commonly used functions like gaussian, exponential, bi-squar can be specified to estimate the weight matrix for the GWR model (Gollini et al., 2015). We selected the gaussian function to estimate the weight matrix and the form of the function is expressed as follows,

$$w_{ij} = exp\left[-\frac{1}{2}\left(\frac{d_{ij}}{b}\right)^2\right] \quad (3)$$

where d_{ij} is the distance between location i and j, b represents the bandwidth (Gollini et al., 2015). Bandwidth is an essential parameter for the GWR model, fixed distance or adaptive distance (fixed number of neighbours) approaches can be used to decide the bandwidth. As the fixed distance suffers from the risk of excessive coefficients in a lower density of observations (Gao et al., 2022), we selected the adaptive approach. To decide the bandwidth, we tested the AICc by varying the bandwidth (number of neighbours) and used 100 as the appropriate bandwidth as it can ensure sufficient observations for local modelling as well as produces relatively low AICc for GWR modelling. The GWR model was implemented using R package "GWmodel" developed by Lu et al. (2022). The evaluation metrics for models (e.g. R^2, adjusted R^2 and AICc) are also computed in the "GWmodel" package. The script for the GWR model is available from GitHub (https://github.com/cherish2019/BiomassUptakeRates) under the GNU General Public Licence v3.0. Local effects of variables on the AGB were visualized and the non-significant polygons for each variable were removed.

2.4.3. Computing the biomass recovery rates, carbon sequestration rates and relative recovery percent

As forest age is a significant variable for secondary forest AGB recovery (Chen et al., 2023) and it has explained approximately half of the variation in AGB of secondary forests in northwest Costa Rica (Becknell & Powers, 2014), we calculate the AGB recovery rates using only forest age variable (log-transformed). We further added STC, which can be derived directly from earth observations with a higher spatial and temporal resolution, in the GWR model to calculate AGB recovery rates locally. Secondary forest polygons that have a non-significant coefficient for any of the input variables were removed, after which, the remained number of secondary forest polygons for GWR models using only forest age and "age + STC" are 27,390 and 25816, respectively. Based on the estimated coefficients from GWR model using forest age and STC, STC was kept constant at the mean while AGB at year 0.01, year 20, and year 34 were predicted. Recover rates of younger (age $\leq$ 20) and older (20 $<$ age $\leq$ 34) secondary forests per polygon were computed as the difference between two predicted AGB values divided by the time interval (number of years). The carbon sequestration rates were calculated by multiplying AGB recovery rates with the IPCC factor of 0.47. We calculated the average AGB for old-growth forests of each biome. Based on recover rates of younger forests computed from GWR model using only forest age, AGB of each polygon was predicted at age 20 and then divided by the mean AGB of old-growth forests in that biome.

3. Results

3.1. Evaluation metrics of OLS and GWR models

The OLS and GWR models were utilized to examine the relationship between the forest AGB and the ten selected predictors. The evaluation metrics of models are shown in Table 2. The adjusted R^2 of using ten selected predictors in the global regression is 0.53, indicating that the percent of variation that can be explained with the ten predictors is 53 %. While for the GWR model, the adjusted R^2 is 0.74. The GWR model explained a larger proportion of variance than the OLS models.

Regarding OLS and GWR models using only forest age, the adjusted R^2 for OLS and GWR models are 0.19 and 0.60, respectively (Table 2).

Table 2
Evaluation metrics of OLS and GWR models.

Models	R^2	Adjusted R^2	AICc
OLS using ten selected variables	0.53	0.53	60663.1
GWR using ten selected variables	0.75	0.74	44967.3
OLS using Age	0.19	0.19	348853.5
GWR using Age	0.60	0.60	328848.0
OLS using Age + STC	0.38	0.38	341247.5
GWR using Age + STC	0.67	0.66	323546.5

Two extra models also have been added to model the AGB and calculate the recovery rates using forest age and STC as explanatory variables, the adjusted R^2 for OLS and GWR models are 0.38 and 0.66, respectively (Table 2). The GWR models explained a larger proportion of variance than the OLS models. The AICc of GWR model also indicates that the GWR model fits better than OLS.

3.2. Coefficients of the OLS and GWR models

3.2.1. OLS model coefficients

The OLS model explores the relationship between the AGB and the selected ten variables. All explanatory variables are statistically significantly related to the response variable, AGB of secondary forests (Table 3).

3.2.2. GWR model coefficients

Regarding GWR model using ten selected variables, the distribution of local R^2, residuals and the coefficients estimates of ten variables are presented in Fig. 3. The spatial distributions of local R^2 show that the goodness of fits at local models in the west, north and southeast of Amazon biome, Cerrado biome, northeast of Atlantic Forest biome, and northeast of Pampa biome is higher. Generally, the Local R^2 is relatively higher at the boundary of different biomes. The effects of different variables on the AGB vary by region. All the variables can have positive or negative effects on the AGB at different locations (Fig. 4). But the proportion of negative and positive effects of the selected variables are different (Fig. 4). Forest age is mainly positively related to the AGB. Especially in the southwest and east of the biome Amazon and the middle of the biome Cerrado, forest age has large effects on the AGB. Regarding CWD, the effects are high in the southwest and northeast of the Amazon biome. The effect of elevation is more significant in the Amazon biome compared with other biomes. In particular, in the west and northeast of this biome, the influence is large. In terms of the influence of fire frequency, positive relationships are mainly found in the Cerrado biome. In the east of the biome Amazon, the positive effect of distance to roads is large. For slope, the effect is highly positively related to AGB in the southwest of the Amazon biome. The positive effect of CEC on the AGB is more significant in Amazon and Atlantic Forest biomes. The positive effect of soil total N is prominent in the south and east of the Amazon biome. While for the effect of STC on the AGB, the effects are larger in the northeast of the Amazon biome and southeast of the Atlantic Forest biome. The effect of tree cover is more prominent in the

Table 3
Statistics of the OLS model using ten selected variables.

Variable	Estimate	Standard error	t value	Pr(>|t|)
Forest age	0.26	0.004	58.56	< 0.001
Climatic water deficit (CWD)	−0.15	0.005	−30.52	< 0.001
Elevation	−0.06	0.005	−13.04	< 0.001
Fire frequency (1985–2019)	−0.07	0.004	−15.34	< 0.001
Distance to roads	0.09	0.005	19.48	< 0.001
Slope	0.06	0.005	13.52	< 0.001
Soil cation exchange capacity	−0.06	0.005	−11.72	< 0.001
Soil total N	0.02	0.005	3.86	< 0.001
Surrounding tree cover (STC)	0.20	0.005	40.95	< 0.001
Tree cover	0.33	0.005	66.19	< 0.001

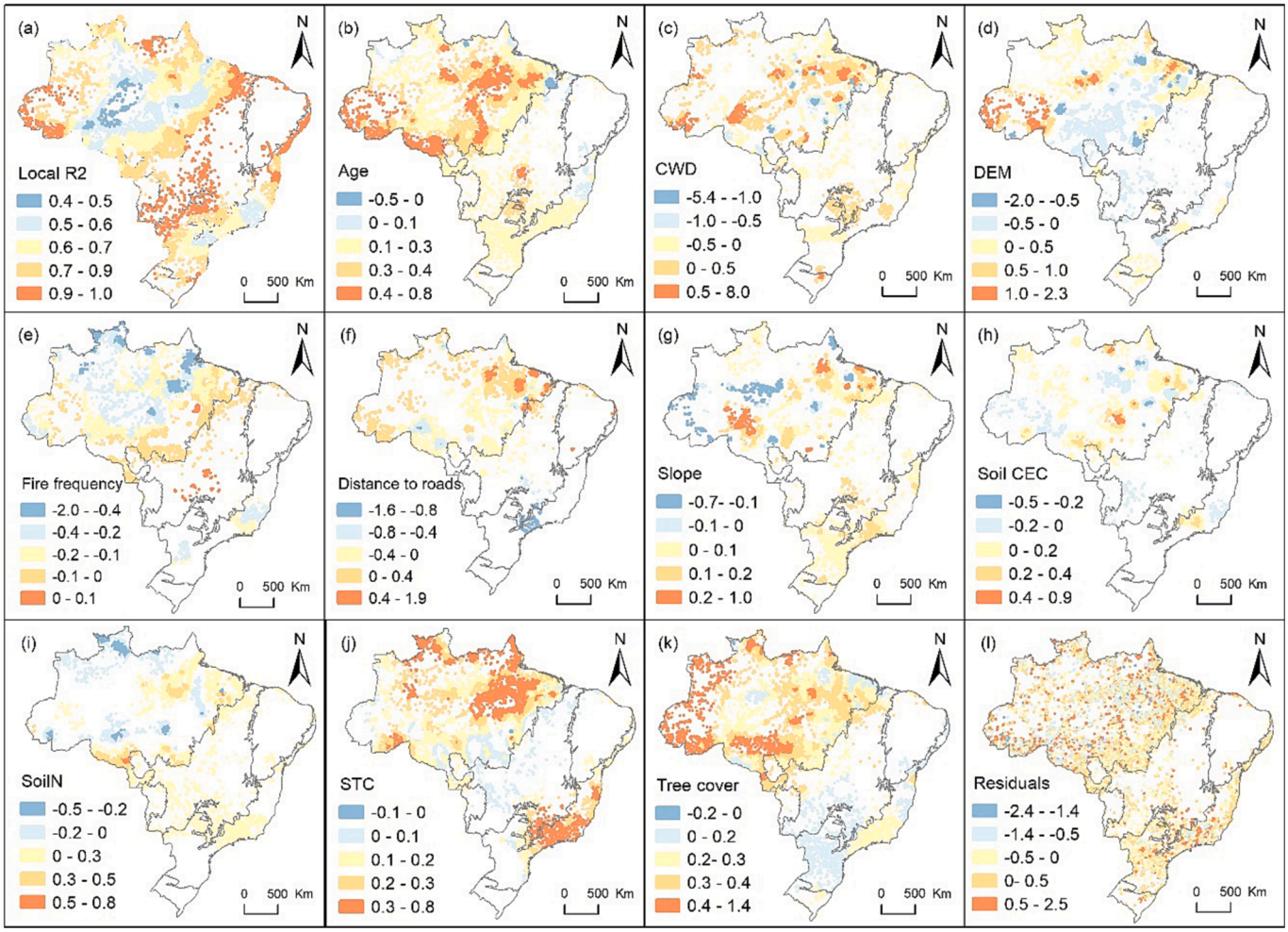

Fig. 3. The distribution of the coefficients of local R^2 (a), each explanatory variable (b-k) and residuals (l) for predicting AGB in secondary forests of Brazil.

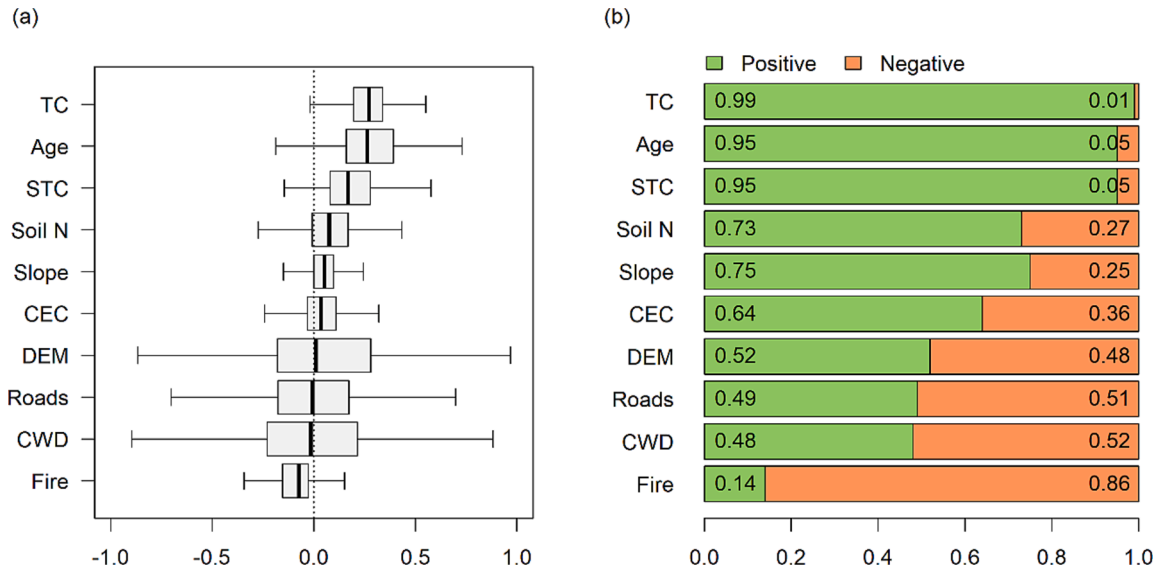

Fig. 4. The distribution of the coefficients estimates (a) and the percentage of positive and negative effects (b) of different variables.

west of the Amazon biome.

The statistical distribution of different estimate coefficients based on the GWR model using the ten selected variables is illustrated in Fig. 4a, the tree cover, forest age and STC are the top 3 variables that positively influence the AGB of secondary forests. Fire frequency was found to mainly has negative effects on AGB. The percentage of positive and negative effects of each variable based on the GWR model are presented in Fig. 4b. Regarding the percent of positive effects of selected factors on

AGB, the tree cover is the highest (99 %). While for the proportion of negative effects of selected factors on AGB, the fire frequency is the highest (86 %), followed by CWD (52 %) and distance to roads (51 %) etc. The distribution of the coefficients estimates and the percentage of positive and effects of different variables for each biome are shown in Supplementary material Figs. 1–2.

3.3. Estimates of AGB recovery rates and carbon sequestration rates

AGB recovery rates were estimated using only forest age as it is one of the most significant variables (Fig. 4). We added STC, another significant variable derived directly from remote sensing data, to estimate the local AGB recovery rates. The coefficient estimates for the STC variable in the GWR model using forest age and STC is shown in Supplementary material Fig. 3. The map of AGB recovery rates shows large variations in different biomes of Brazil in secondary forests (Fig. 4 and Supplementary material Fig. 5). The average AGB recovery rates of each biome range from 4.2 Mg ha^{-1} yr^{-1} to 7.8 Mg ha^{-1} yr^{-1} based on the GWR model using forest age variable (Table 4). The average AGB recovery rates of each biome of GWR model using forest age and STC are shown in Supplementary material Table 2.

Among all biomes of Brazil, the average recovery rate of the Biome Amazon is the largest, the Caatinga biome is the smallest in the young secondary forests (Table 4). A similar trend can be found in the old secondary forests across all biomes. The average recovery rate for all young secondary forests is approximately 4 times of the recovery rate for all old secondary forests in Brazil. The carbon sequestration rates of secondary forests vary spatially in the secondary forests of Brazil (Supplementary material Figs. 4 & 5). The average carbon sequestration rates for each biome in Brazil are shown in Supplementary material Table 3.

Generally, the spatial patterns of AGB recovery estimated from forest age only and "forest age + STC" models are similar, and the AGB recovery rates estimated from the forest age only model are larger than those estimated from the "forest age + STC" model (Fig. 5 and Supplementary material Fig. 5).

The relative recovery percentage varies significantly across different regions within the Amazon biome and Atlantic Forest biome, as depicted in Fig. 6. Within the Amazon biome, the rate of relative recovery is comparatively slower in the middle, northwest, and southeast regions. On the other hand, in the Atlantic Forest biome, the relative recovery is slower in the northeast region. These spatial variations highlight the heterogeneity in the recovery processes and suggest that different areas within these biomes have distinct patterns of AGB recovery. The average relative recovery percentage for the Caatinga, Cerrado, Pampa, and Pantanal biomes surpasses 100 %, indicating that the recovery of these biomes will exceed their original state after 20 years. In contrast, the remaining biomes have average relative recovery percentages lower than 100 %, implying that AGB recovery has not yet reached or surpassed their initial conditions after 20 years.

Table 4
Average AGB recovery rates for each biome based on the GWR model using forest age.

	AGB recovery rates (Mg ha^{-1} yr^{-1}) using forest age	
	Age ≤ 20	20 < Age ≤ 34
All	7.47	1.83
Amazon	7.77	1.90
Caatinga	4.20	1.03
Cerrado	6.30	1.54
Atlantic Forest	5.46	1.34
Pampa	5.13	1.26
Pantanal	6.72	1.65

4. Discussion

We explored how selected variables (e.g., forest age, STC, fire frequency) influence the AGB of secondary forests locally and estimate the local AGB recovery rates. Our results show that the different variables' influence on secondary forests AGB varies in space. Generally, tree cover, forest age and STC are the three main drivers of AGB. Tree cover, forest age, STC, Soil N, Slope, and CEC mainly positively related to AGB, which aligns with previous research (Oberleitner et al., 2021; Pugh et al., 2019; Chen et al., 2023). Fire mainly has a negative effect on AGB, consistent with research conducted in tropical forests (Martins et al., 2012; Slik et al., 2008). Regarding elevation, distance to nearest roads and CWD, the percentage of positive and negative effects are similar (Fig. 4). The large proportion of the elevation has positive effects on the AGB is difficult to explain (Fig. 4). Unexpectedly, we did not find a clear positive relationship between distance to roads and AGB. We expect elevation to be negatively associated with AGB (Maza et al., 2022). Higher AGB is associated with higher water availability (lower CWD) (Poorter et al., 2016). The percentage of positive and negative effects of the CWD on AGB is similar, which might be explained by the fact that the effect of climate on the AGB in tropical regions varies by space and might be scale-dependent (Álvarez-Dávila et al., 2017).

Based on the estimated AGB recovery rates from the forest age model, our estimated average rates for younger secondary forests in each biome (except biome Pampa) (Table 4) are on average 17.7 % larger than those of the IPCC default AGB change rates (IPCC, 2019). The comparison between IPCC default rates and our estimated recovery rates using forest age and "forest age + STC" models are shown in Fig. 8 and Supplementary material Fig. 4. As the extent of the biomes used in the present study and the global ecozones used in IPCC are different, the ecozone map was overlayed with the biome map to identify the main ecozone for each biome. Amazon biome and Caatinga biome are compared with the tropical rainforest and tropical dry forests in the Americas, respectively. Cerrado and Pantanal biomes are compared with tropical moist forests in the Americas. Atlantic Forest was compared with the average of two ecozones (tropical rainforest and tropical moist forest). The Pampa biome is not compared since it mainly overlays with the subtropical humid forest, for which a 2019 IPCC default rate for secondary forests was not derived. Our estimated local recovery rates are generally consistent with the IPCC rates, with most falling within two standard deviations of the mean compared. The small discrepancy between the estimated mean recovery rates and IPCC default values in each biome (Fig. 8), suggests that our estimated recovery rates were comparable with IPCC default values. Local AGB recovery rates can provide spatially explicit information about the carbon sequestration potential of secondary forests and thus provide important complementary information that enables the IPCC to refine the estimates accordingly.

Our estimated local recovery rates map (Fig. 5) provides spatially explicit information that complements our understanding of forest carbon stocks. Our secondary forest AGB recovery rates map captures more than 31.3-fold variations, approximately three times compared with previous research conducted in Neotropical secondary forests (Poorter et al., 2016). By illustrating the variation in recovery rates across different regions, the map enhances the capability of identifying areas where carbon sequestration efforts may be most effective. Results from previous studies that utilized 13,112 georeferenced ground measurements revealed similar trends (Cook-Patton et al., 2020). Brazil's carbon sequestration rate estimated from GWR based on the forest age model (3.51 Mg C/ha yr^{-1}) is close to previous studies that combine filed data and remote sensing data (Poorter et al., 2016). For example, a previous study used 1500 forest plots and combined that with variables derived from remote sensing products to study the recovery rates in Neotropics and the estimated carbon uptake rate was 3.05 Mg C ha^{-1} yr^{-1} (Poorter et al., 2016), which is marginally lower than our estimated rate.

Our findings for the Brazilian Amazon corroborate previous studies,

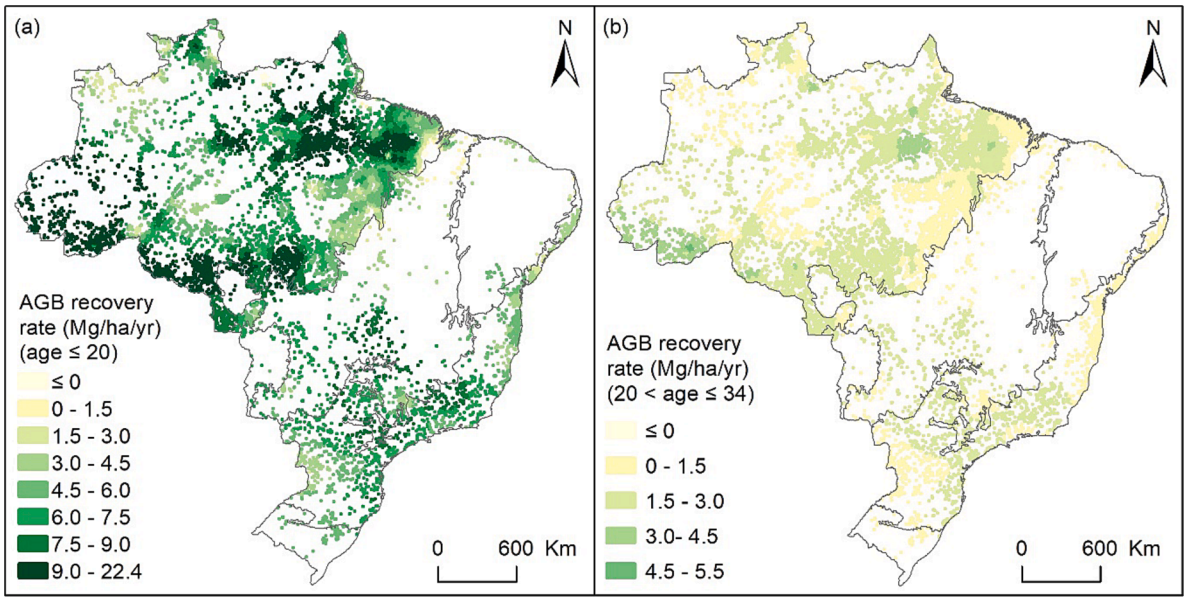

Fig. 5. AGB recovery rates of younger and older secondary forests based on GWR using only forest age.

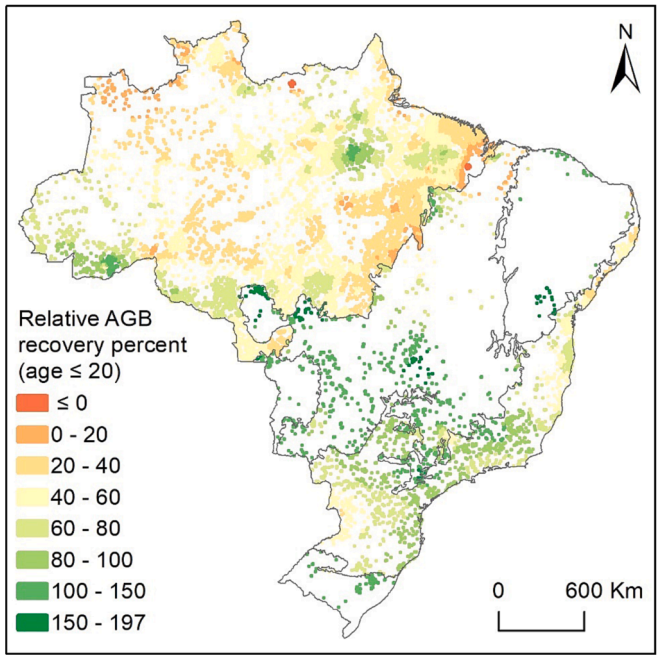

Fig. 6. Relative AGB recovery percent of younger secondary forests at age = 20 based on GWR using only forest age.

which demonstrated a remarkable variability in the capacity of secondary forests to uptake atmospheric carbon (Elias et al., 2020; Heinrich et al., 2021). Furthermore, we discovered this variability was repeated within and between other Brazilian biomes. Thus, the variation in environmental characteristics throughout Brazil can explain the variability of recovery factors. The structure and composition of previously deforested mature forests or the surrounding remnants (which vary between the biomes) will determine the species and the abundance of the seed bank available for the recovery process of secondary forests and, consequently, the carbon accumulation rates (Baider et al., 2001; Poorter et al., 2016). In the Amazon, Cerrado and Atlantic Forest (mature forests with greater carbon storage capacity), recovery rates were higher than in the Caatinga (mature forests with lower carbon storage capacity). Cloud cover determines the amount of diffuse solar radiation available on the ground; diffuse radiation can penetrate deeper into closed forest canopies than direct radiation and enhance productivity and carbon accumulation rate (Mercado et al., 2009; Roderick et al., 2001). Thus, this can explain why biomes such as Amazon, Cerrado and Atlantic Forest (high-level cloud coverage) have higher recovery rates than other biomes (Martins et al., 2018). Hydroclimatic conditions are other important factors that control recovery rates - drier biomes showed lower recovery rates than biomes with greater water availability. Furthermore, drier forests are more susceptible to fire, a disturbance that can reduce the recovery capacity of secondary forests by 40 % to 50 % (Heinrich et al., 2021; Zarin et al., 2005). In addition to these factors, the combination of different distributions of characteristics such as elevation, slope, and soil type can also explain the variability of recovery rates found here, as they will determine the limitation of recovery rates (Chazdon et al., 2016; Heinrich et al., 2021; Poorter et al.,

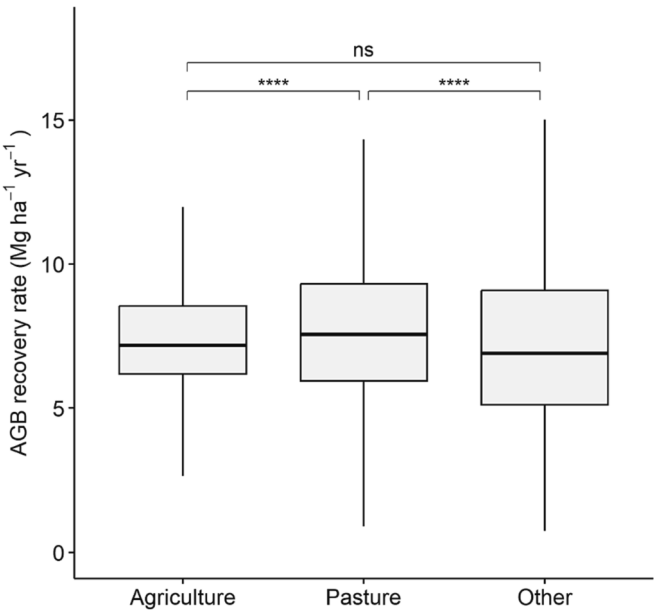

Fig. 7. Comparison between the AGB recovery rates among different previous land use types. "****" indicates that P ≤ 0.0001 and "ns" represent P > 0.05.

2021, 2016). Previous land use could also affect the AGB recovery rates (Fig. 7), but its local effects on AGB recovery rates need further investigation. The AGB recovery rates depend on a combination of local environmental conditions, ecological processes, and human influences. The North-South variations in the Atlantic Forest biome might be explained by the difference in the tree cover and surrounding tree cover, which is related to seed abundance. The variation of AGB recovery rates in the Amazon biome could also explained by the difference in the forest age, tree cover, soil fertility water availability, etc. For example, the surprisingly low recovery rate of the Cabeça de Cachorro (Amazonas state) areas might be explained by that the forest age of secondary forests in that region is relatively higher than in other regions.

Exploring AGB recovery using geospatial data has many challenges. Firstly, the distribution of residuals and the relatively low R^2 indicates that a significant proportion of the variance remains unexplained. Future work needs to investigate the potential of adding other variables, such as previous land use, and disturbance intensity/history for improving the performance of estimating AGB recovery rates. Previous land use /land cover (LUCC) types of different secondary forest polygons based on LUCC maps provided by the MapBiomas Project (MapBiomas Collection 6) (Souza et al., 2020). We used one-way analysis of variance (ANOVA) to determine whether there are any statistically significant differences between the mean AGB recovery rates of younger secondary forests of three different previous land use groups, including agriculture, pasture, and other land use types. We selected these three land use types because large amounts of forests have been changed into mainly agriculture and pastures in the tropics (Jakovac et al., 2021). The results show that there is a significant difference between the mean AGB recovery rates of younger secondary forests of these three different previous land use types ($P < 0.05$, Fig. 7). However, the local effects of previous land use type on the AGB recovery is difficult to analyze as previous land use is categorical variables and it clusters spatially, there is a high risk of encountering local multicollinearity while integrating categorical variable into GWR model (Liu et al., 2017). Besides, a previous study has revealed that regrowth rates exposed to more than 3 times of deforestation prior to regrowth were lower compared with those experiencing one deforestation in the Brazilian Amazon (Heinrich et al., 2021). Thus, it is necessary to integrate previous land use and disturbance intensity /history for characterizing the secondary forest recovery in future research. Secondly, the input data might cause certain circularity in the models. For example, CEC and Soil total Nitrogen derived from the SoilGrids 2.0 data used original bands and vegetation indices derived from Landsat images (Poggio et al., 2021), while forest age and fire also derived from Landsat imagery. Thirdly, the spatial distribution and uncertainty in forest age maps also contribute to the errors of our models. Younger secondary forests (less than 5 years old) clustered in the east of the Amazon biome, low variation in the forest age distribution could reduce the accuracy of the models as its estimation of recovery rates highly depends on the very young secondary forests. This might explain the negative recovery rates and negative effects of forest age because older forests have relatively lower AGB than younger forests. Fourthly, using the global biomass data for local analysis is challenging, replacing the global biomass map with a regional one might have the potential to improve the estimation of AGB recovery. Future research could explore the potential of mapping aboveground biomass based on LiDAR data collected by the "improving biomass estimation methods for the Amazon" (EBA) project conducted by the National Institute for Space Research (INPE) (Ometto et al., 2021) or using the regional AGB map (Ometto et al., 2023). Next, bandwidth is an essential parameter for GWR, although we used the adaptive approach for specifying the bandwidth, it is still unavoidable that the local model may use observations that are further away from each other. Then, the AGB recovery rates estimated from the age and STC model are generally lower than those estimated from the forest age model. This suggests that AGB

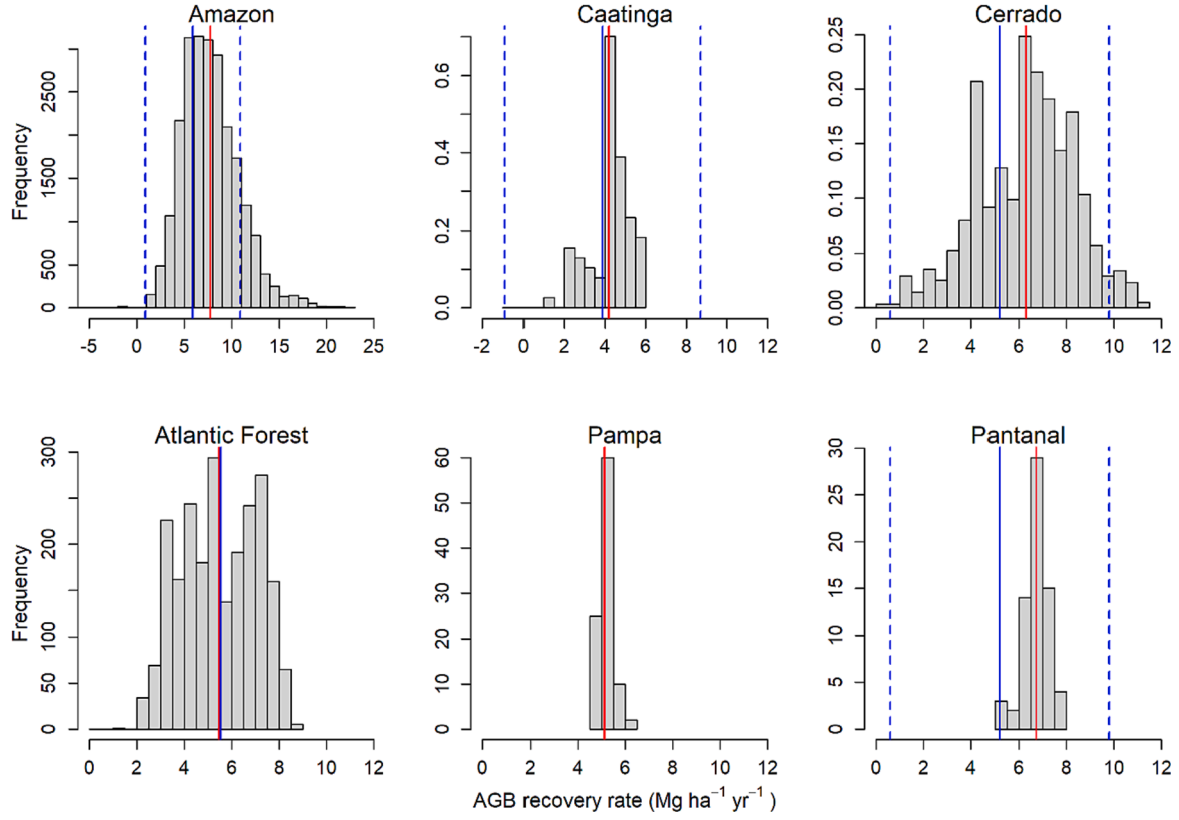

Fig. 8. Comparing the AGB recovery rates estimated from forest age with IPCC default rates. The vertical red line represents the mean AGB recovery rate of each biome. The blue solid line and blue dashed line represent the mean and 2 standard deviations from the mean IPCC default rates, respectively. (For interpretation of the references to colour in this figure legend, the reader is referred to the web version of this article.)

recovery rates estimated from age and STC may be underestimated as the STC was held constant and was subtracted when subtracting the AGB at year 0.01. Furthermore, the use of various geospatial datasets collected in different years introduced uncertainty in models, for example, the AGB map was acquired in 2018, while the tree cover map and distance to settlements and roads were acquired in 2019 and acquired in 2021, respectively. Future research could explore the potential of characterizing AGB recovery rates using datasets acquired from the same year when they are available. Finally, the results of GWR models were not validated due to unavailable field data. Integrating field data or LiDAR data could have the potential to improve our results. For instance, a previous study has illustrated the potential of combining field measurements and LiDAR to estimate the AGB in tropical secondary forests (Jha et al., 2020).

Our results provide complementary information by providing spatially explicit recovery rate maps. Moreover, our results have the potential of capturing more variations of the varied AGB recovery rates of secondary forests, thus providing important information for reducing the uncertainty related to quantifying the climate mitigation potential and terrestrial carbon stocks of secondary forests at a national scale. Our framework for estimating local AGB recovery rates could also be tested in other tropical countries if forest age data is available.

5. Conclusions

We assessed the spatial effects of selected factors on secondary forests in Brazil, finding that forest age and tree cover are the main predictors for characterizing AGB secondary forests in Brazil. All the variables could have positive or negative effects on the AGB at a local scale, with spatially varying magnitudes. We presented AGB and carbon sequestration recovery rates maps that illustrate the geographic variation in the climate mitigation potential of secondary forests in Brazil. The estimated secondary forests AGB recovery rates (using forest age) varied more than 31.3-fold across sites. Our analysis provides crucial information for understanding the AGB resilience spatially and serves as a basis for quantifying the climate mitigation potential of regrowing forests at the country scale. Additionally, our estimated AGB recovery rates provide spatially explicit information for policymakers to develop sustainable forest management strategies. For example, our maps could assist Brazil in monitoring or evaluating its progress towards National Determined Contributions (NDCs) targets to the UNFCCC. Our analysis could serve as a basis for estimating local secondary forest AGB recovery rates in other tropical countries. Extra attention could be paid to the conservation of forests in regions with slow recovery. Afforestation initiatives also could take advantage of these recovery rate maps and arrange activities in regions with high recovery rates. Finally, our results can reduce uncertainties in MRV (Measuring, Reporting and Verifying) systems in jurisdictional and voluntary REDD+ (Reducing emissions from deforestation and forest degradation) programs in the carbon market. Due to its continental dimensions, obtaining carbon uptake rates from field approaches for secondary forests in Brazil is impracticable. Thus, our uptake rates map based on remote sensing data provides an unprecedented database to meet the needs of REDD + programs developed in the country.

Declaration of competing interest

The authors declare that they have no known competing financial interests or personal relationships that could have appeared to influence the work reported in this paper.

Acknowledgements

This project is be supported by the China Scholarship Council (No. 201907720098), the CCI Biomass Phase 2 projects & GFOI R&D office (funded by ESA), the CGIAR MITIGATE+ project and WRI land and carbon lab. We gratefully acknowledge the support of Wallace Vieira da Silva and Arnan Araza for accessing the fire frequency data in Brazil and downloading global AGB maps, respectively. C.H.L.S-J was supported by the University of Manchester through the “Forest fragmentation mapping of Amazon and its vulnerable margin Amazon-Cerrado transition forests” project, the National Council for Scientific and Technological Development - CNPq (grant 401741/2023-0). The authors are willing to share the data and scripts upon request.

Appendix A. Supplementary data

Supplementary data to this article can be found online at https://doi.org/10.1016/j.isprsjprs.2023.12.013.

References

Abatzoglou, J.T., Dobrowski, S.Z., Parks, S.A., Hegewisch, K.C., 2017. Data Descriptor : TerraClimate, a high-resolution global dataset of monthly climate and climatic water balance from 1958–2015. Sci. Data 5, 170191. https://doi.org/10.1038/sdata.2017.191.

Ahmed, R., Siqueira, P., Hensley, S., 2013. A study of forest biomass estimates from lidar in the northern temperate forests of New England. Remote Sens. Environ. 130, 121–135. https://doi.org/10.1016/j.rse.2012.11.015.

Alencar, A.A.C., Arruda, V.L.S., da Silva, W.V., Conciani, D.E., Costa, D.P., Crusco, N., Duverger, S.G., Ferreira, N.C., Franca-Rocha, W., Hasenack, H., Martenexen, L.F.M., Piontekowski, V.J., Ribeiro, N.V., Rosa, E.R., Rosa, M.R., dos Santos, S.M.B., Shimbo, J.Z., Vélez-Martin, E., 2022. Long-Term Landsat-Based Monthly Burned Area Dataset for the Brazilian Biomes Using Deep Learning. Remote Sens. (Basel) 14 (11). https://doi.org/10.3390/rs14112510.

Álvarez-Dávila, E., Cayuela, L., González-Caro, S., Aldana, A.M., Stevenson, P.R., Phillips, O., Cogollo, Á., Peñuela, M.C., von Hildebrand, P., Jiménez, E., Melo, O., Londoño-Vega, A.C., Mendoza, I., Velásquez, O., Fernández, F., Serna, M., Velázquez-Rua, C., Benítez, D., Rey-Benayas, J.M., 2017. Forest biomass density across large climate gradients in northern South America is related to water availability but not with temperature. PLoS One 12 (3). https://doi.org/10.1371/journal.pone.0171072.

Araza, A., de Bruin, S., Herold, M., Quegan, S., Labriere, N., Rodriguez-Veiga, P., Avitabile, V., Santoro, M., Mitchard, E.T.A., Ryan, C.M., Phillips, O.L., Willcock, S., Verbeeck, H., Carreiras, J., Hein, L., Schelhaas, M.-J., Pacheco-Pascagaza, A.M., da Conceição Bispo, P., Laurin, G.V., Lucas, R., 2022. A comprehensive framework for assessing the accuracy and uncertainty of global above-ground biomass maps. Remote Sens. Environ. 272, 112917 https://doi.org/10.1016/j.rse.2022.112917.

Baider, C., Tabarelli, M., Mantovani, W., 2001. The soil seed bank during Atlantic Forest regeneration in Southeast Brazil. Braz. J. Biol. 61 (1), 35–44. https://doi.org/10.1590/S0034-71082001000100006.

Justin M. Becknell, Michael Keller, Daniel Piotto, M. L., & Rodrigo Bruno de Oliveira Cavalcante, and S. P. (2018). *Landscape-scale lidar analysis of aboveground biomass distribution in secondary Brazilian*.

Becknell, J.M., Powers, J.S., 2014. Stand age and soils as drivers of plant functional traits and aboveground biomass in secondary tropical dry forest. Can. J. For. Res. 44 (6), 604–613. https://doi.org/10.1139/cjfr-2013-0331.

Brunsdon, C., Fotheringham, A.S., Charlton, M.E., 1996. Geographically weighted regression: a method for exploring spatial nonstationarity. Geogr. Anal. 28 (4), 281–298. https://doi.org/10.1111/j.1538-4632.1996.tb00936.x.

Buchhorn, M., Lesiv, M., Tsendbazar, N.E., Herold, M., Bertels, L., Smets, B., 2020. Copernicus global land cover layers-collection 2. Remote Sens. (Basel) 12 (6). https://doi.org/10.3390/rs12061044.

Cardozo, O.D., García-Palomares, J.C., Gutiérrez, J., 2012. Application of geographically weighted regression to the direct forecasting of transit ridership at station-level. Appl. Geogr. 34, 548–558. https://doi.org/10.1016/j.apgeog.2012.01.005.

César, R.G., de S. Moreno, V., Coletta, G.D., Schweizer, D., Chazdon, R.L., Barlow, J., Ferraz, S.F.B., Crouzeilles, R., Brancalion, P.H.S., 2021. It is not just about time: Agricultural practices and surrounding forest cover affect secondary forest recovery in agricultural landscapes. Biotropica 53 (2), 496–508. https://doi.org/10.1111/btp.12893.

Chao, L., Zhang, K., Li, Z., Zhu, Y., Wang, J., Yu, Z., 2018. Geographically weighted regression based methods for merging satellite and gauge precipitation. J. Hydrol. 558, 275–289. https://doi.org/10.1016/j.jhydrol.2018.01.042.

Chazdon, R.L., Broadbent, E.N., Rozendaal, D.M.A., Bongers, F., Zambrano, A.M.A., Aide, T.M., Balvanera, P., Becknell, J.M., Boukili, V., Brancalion, P.H.S., Craven, D., Almeida-Cortez, J.S., Cabral, G.A.L., de Jong, B., Denslow, J.S., Dent, D.H., DeWalt, S.J., Dupuy, J.M., Durán, S.M., Espírito-Santo, M.M., Fandino, M.C., César, R.G., Hall, J.S., Hernández-Stefanoni, J.L., Jakovac, C.C., Junqueira, A.B., Kennard, D., Letcher, S.G., Lohbeck, M., Martínez-Ramos, M., Massoca, P., Meave, J. A., Mesquita, R., Mora, F., Muñoz, R., Muscarella, R., Nunes, Y.R.F., Ochoa-Gaona, S., Orihuela-Belmonte, E., Peña-Claros, M., Pérez-García, E.A., Piotto, D., Powers, J.S., Rodríguez-Velazquez, J., Romero-Pérez, I.E., Ruíz, J., Saldarriaga, J.G., Sanchez-Azofeifa, A., Schwartz, N.B., Steininger, M.K., Swenson, N.G., Uriarte, M., van Breugel, M., van der Wal, H., Veloso, M.D.M., Vester, H., Vieira, I.C.G., Bentos, T.V., Williamson, G.B., Poorter, L., 2016. Carbon sequestration potential of

second-growth forest regeneration in the Latin American tropics. Sci. Adv. 2 (5), e1501639. https://doi.org/10.1126/sciadv.1501639.
Chen, N., Tsendbazar, N.E., Requena Suarez, D., Verbesselt, J., Herold, M., 2023. Characterizing aboveground biomass and tree cover of regrowing forests in Brazil using multi-source remote sensing data. Remote Sens. Ecol. Conserv. 9 (4), 553–567.
Chokkalingam, U., De Jong, W., 2001. Secondary forest: a working definition and typology. Int. For. Rev. 3 (1), 19–26.
Cook-Patton, S.C., Leavitt, S.M., Gibbs, D., Harris, N.L., Lister, K., Anderson-Teixeira, K. J., Briggs, R.D., Chazdon, R.L., Crowther, T.W., Ellis, P.W., Griscom, H.P., Herrmann, V., Holl, K.D., Houghton, R.A., Larrosa, C., Lomax, G., Lucas, R., Madsen, P., Malhi, Y., Griscom, B.W., 2020. Mapping carbon accumulation potential from global natural forest regrowth. Nature 585 (7826), 545–550. https://doi.org/10.1038/s41586-020-2686-x.
Crk, T., Uriarte, M., Corsi, F., Flynn, D., 2009. Forest recovery in a tropical landscape: What is the relative importance of biophysical, socioeconomic, and landscape variables? Landsc. Ecol. 24 (5), 629–642. https://doi.org/10.1007/s10980-009-9338-8.
David, R.M., Rosser, N.J., Donoghue, D.N.M., 2022. Improving above ground biomass estimates of Southern Africa dryland forests by combining Sentinel-1 SAR and Sentinel-2 multispectral imagery. Remote Sens. Environ. 282 https://doi.org/10.1016/j.rse.2022.113232.
De Castro, A.P., Da Silva, M.R.S.S., Quirino, B.F., Da Cunha Bustamante, M.M., Krüger, R. H., 2016. Microbial diversity in cerrado biome (neotropical savanna) soils. PLoS One 11 (2). https://doi.org/10.1371/journal.pone.0148785.
de Keersmaecker, W., Rodríguez-Sánchez, P., Milencović, M., Herold, M., Reiche, J., Verbesselt, J., 2022. Evaluating recovery metrics derived from optical time series over tropical forest ecosystems. Remote Sens. Environ. 274 https://doi.org/10.1016/j.rse.2022.112991.
Decuyper, M., Chávez, R.O., Lohbeck, M., Lastra, J.A., Tsendbazar, N., Hackländer, J., Herold, M., Vågen, T.G., 2022. Continuous monitoring of forest change dynamics with satellite time series. Remote Sens. Environ. 269 https://doi.org/10.1016/j.rse.2021.112829.
DeVries, B., Decuyper, M., Verbesselt, J., Zeileis, A., Herold, M., Joseph, S., 2015. Tracking disturbance-regrowth dynamics in tropical forests using structural change detection and Landsat time series. Remote Sens. Environ. 169, 320–334. https://doi.org/10.1016/j.rse.2015.08.020.
Dziauddin, M.F., Powe, N., Alvanides, S., 2015. Estimating the Effects of Light Rail Transit (LRT) System on Residential Property Values Using Geographically Weighted Regression (GWR). Appl. Spat. Anal. Policy 8 (1), 1–25. https://doi.org/10.1007/s12061-014-9117-z.
Elias, F., Ferreira, J., Lennox, G.D., Berenguer, E., Ferreira, S., Schwartz, G., de O. Melo, L., Reis Júnior, D.N., Nascimento, R.O., Ferreira, F.N., Espirito-Santo, F., Smith, C.C., Barlow, J., 2020. Assessing the growth and climate sensitivity of secondary forests in highly deforested Amazonian landscapes. Ecology 101 (3), e02954.
Farr, T. G., Rosen, P. A., Caro, E., Crippen, R., Duren, R., Hensley, S., … Alsdorf, D., 2007. The Shuttle Radar Topography Mission. Rev. Geophys. 45, RG 2004. https://doi.org/10.1029/2005RG000183.
Fotheringham, A.S., Brunsdon, C., Charlton, M., 2002. Geographically weighted regression: the analysis of spatially varying relationships. Wiley, Chichester.
Gao, Y., Zhao, J., Han, L., 2022. Exploring the spatial heterogeneity of urban heat island effect and its relationship to block morphology with the geographically weighted regression model. Sustain. Cities Soc. 76 https://doi.org/10.1016/j.scs.2021.103431.
Ge, Y., Song, Y., Wang, J., Liu, W., Ren, Z., Peng, J., Lu, B., 2017. Geographically weighted regression-based determinants of malaria incidences in northern China. Trans. GIS 21 (5), 934–953. https://doi.org/10.1111/tgis.12259.
I. Gollini B. Lu M. Charlton C. Brunsdon P. Harris GWmodel: An R Package for Exploring Spatial Heterogeneity Using Geographically Weighted Models. In JSS Journal of Statistical Software 63 2015 10.18637/jss.v063.i17.
Heinrich, V.H.A., Dalagnol, R., Cassol, H.L.G., Rosan, T.M., de Almeida, C.T., Silva Junior, C.H.L., Campanharo, W.A., House, J.I., Sitch, S., Hales, T.C., Adami, M., Anderson, L.O., Aragão, L.E.O.C., 2021. Large carbon sink potential of secondary forests in the Brazilian Amazon to mitigate climate change. Nature Communications 12 (1). https://doi.org/10.1038/s41467-021-22050-1.
Heinrich, V.H.A., Vancutsem, C., Dalagnol, R., Rosan, T.M., Fawcett, D., Silva-Junior, C. H.L., Cassol, H.L.G., Achard, F., Jucker, T., Silva, C.A., House, J., Sitch, S., Hales, T. C., Aragão, L.E.O.C., 2023. The carbon sink of secondary and degraded humid tropical forests. Nature 615 (7952), 436–442. https://doi.org/10.1038/s41586-022-05679-w.
IPCC (2019). 2019 Refinement to the 2006 IPCC Guidelines for National Greenhouse Gas Inventories: In D Blain et al. (Eds), Vol 4 Chapter 4 Forest Land. Japan: IGES, https://www.ipccnggip.iges.or.jp/public/2019rf/pdf/4_Volume4/19R_V4_Ch04_Forest%20Land.pdf.
Ivory, S.J., McGlue, M.M., Spera, S., Silva, A., Bergier, I., 2019. Vegetation, rainfall, and pulsing hydrology in the Pantanal, the world's largest tropical wetland. Environ. Res. Lett. 14 (12) https://doi.org/10.1088/1748-9326/ab4ffe.
Jakovac, C.C., Junqueira, A.B., Crouzeilles, R., Peña-Claros, M., Mesquita, R.C.G., Bongers, F., 2021. The role of land-use history in driving successional pathways and its implications for the restoration of tropical forests. Biol. Rev. 96 (4), 1114–1134. https://doi.org/10.1111/brv.12694.
Jha, N., Kumar Tripathi, N., Chanthorn, W., Brockelman, W., Nathalang, A., Pelissier, R.-M., M., 2020. Forest aboveground biomass stock and resilience in a tropical landscape of Thailand. Biogeosciences 17 (1), 121–134. https://doi.org/10.5194/bg-17-121-2020.
Jin, C., Xu, J., Huang, Z., 2019. Spatiotemporal analysis of regional tourism development: A semiparametric Geographically Weighted Regression model approach. Habitat International 87, 1–10. https://doi.org/10.1016/j.habitatint.2019.03.011.
Kang, L., Di, L., Deng, M., Shao, Y., Yu, G., Shrestha, R., 2014. Use of geographically weighted regression model for exploring spatial patterns and local factors behind NDVI-precipitation correlation. IEEE J. Sel. Top. Appl. Earth Obs. Remote Sens. 7 (11), 4530–4538. https://doi.org/10.1109/JSTARS.2014.2361128.
Li, C., Li, Y., Li, M., 2019. Improving forest aboveground biomass (AGB) estimation by incorporating crown density and using Landsat 8 OLI images of a subtropical forest in western Hunan in central China. Forests 10 (2). https://doi.org/10.3390/f10020104.
Liu, C., Rong, W., Yan, J., Reid, K.B., 2017. Exploring non-stationary and scale-dependent relationships between walleye (Sander vitreus) distribution and habitat variables in Lake Erie. Marine & Freshwater Research 68, 270–281. https://doi.org/10.1071/MF15374.
Lu, D., 2006. The potential and challenge of remote sensing-based biomass estimation. Int. J. Remote Sens. 27 (7), 1297–1328. https://doi.org/10.1080/01431160500486732.
Lu, B., Charlton, M., Fotheringham, A.S., 2011. Geographically Weighted Regression using a non-Euclidean distance metric with a study on London house price data. Procedia Environ. Sci. 7, 92–97. https://doi.org/10.1016/j.proenv.2011.07.017.
Lu, B., Charlton, M., Harris, P., Fotheringham, A.S., 2014. Geographically weighted regression with a non-Euclidean distance metric: A case study using hedonic house price data. Int. J. Geogr. Inf. Sci. 28 (4), 660–681. https://doi.org/10.1080/13658816.2013.865739.
Lu, B., Hu, Y., Murakami, D., Brunsdon, C., Comber, A., Charlton, M., Harris, P., 2022. High-performance solutions of geographically weighted regression in R. Geo-Spatial Information Science 25 (4), 536–549. https://doi.org/10.1080/10095020.2022.2064244.
Mackey, B., DellaSala, D.A., Kormos, C., Lindenmayer, D., Kumpel, N., Zimmerman, B., Hugh, S., Young, V., Foley, S., Arsenis, K., Watson, J.E.M., 2015. Policy Options for the World's Primary Forests in Multilateral Environmental Agreements. Conserv. Lett. 8 (2), 139–147. https://doi.org/10.1111/conl.12120.
Martins, V.S., Novo, E.M.L.M., Lyapustin, A., Aragão, L.E.O.C., Freitas, S.R., Barbosa, C. C.F., 2018. Seasonal and interannual assessment of cloud cover and atmospheric constituents across the Amazon (2000–2015): Insights for remote sensing and climate analysis. ISPRS J. Photogramm. Remote Sens. 145, 309–327. https://doi.org/10.1016/j.isprsjprs.2018.05.013.
Martins, F.S.R.V., Xaud, H.A.M., dos Santos, J.R., Galvão, L.S., 2012. Effects of fire on aboveground forest biomass in the northern Brazilian Amazon. J. Trop. Ecol. 28 (6), 591–601. https://doi.org/10.1017/S0266467412000636.
Maza, B., Rodes-Blanco, M., Rojas, E., 2022. Aboveground Biomass Along an Elevation Gradient in an Evergreen Andean-Amazonian Forest in Ecuador. Frontiers in Forests and Global Change 5. https://doi.org/10.3389/ffgc.2022.738585.
Mercado, L.M., Bellouin, N., Sitch, S., Boucher, O., Huntingford, C., Wild, M., Cox, P.M., 2009. Impact of changes in diffuse radiation on the global land carbon sink. Nature 458, 1014–1017. https://doi.org/10.1038/nature07949.
Oberleitner, F., Egger, C., Oberdorfer, S., Dullinger, S., Wanek, W., Hietz, P., 2021. Recovery of aboveground biomass, species richness and composition in tropical secondary forests in SW Costa Rica. Forest Ecology and Management 479, 118580. https://doi.org/10.1016/j.foreco.2020.118580.
Ometto, J.P., Gorgens, B.G., Assis, M., Cantinho, R.Z., de S. Pereira, F.R., Sato, L.Y., 2021. Summary of the Airborne LiDAR transects collected by EBA in the Brazilian Amazon (Version 20210223). Zenodo. https://doi.org/10.5281/zenodo.4557390.
Ometto, J.P., Gorgens, E.B., de Souza Pereira, F.R., Sato, L., de Assis, M.L.R., Cantinho, R., Longo, M., Jacon, A.D., Keller, M., 2023. A biomass map of the Brazilian Amazon from multisource remote sensing. Sci. Data 10 (1), 668. https://doi.org/10.1038/s41597-023-02575-4.
OpenStreetMap Contributors, OpenStreetMap. Available online: http://download.geofabrik.de/south-america/brazil.html (accessed on November 12, 2021).
Orihuela-Belmonte, D.E., De Jong, B.H.J., Mendoza-Vega, J., Van der Wal, J., Paz-Pellat, F., Soto-Pinto, L., Flamenco-Sandoval, A., 2013. Carbon stocks and accumulation rates in tropical secondary forests at the scale of community, landscape and forest type. Agr Ecosyst Environ 171, 72–84. https://doi.org/10.1016/j.agee.2013.03.012.
Pain, A., Marquardt, K., Lindh, A., Hasselquist, N.J., 2021. What is secondary about secondary tropical forest? Rethinking forest landscapes. Human Ecol. 49 (3), 239–247. https://doi.org/10.1007/s10745-020-00203-y.
Pasculli, A., Palermi, S., Sarra, A., Piacentini, T., Miccadei, E., 2014. A modelling methodology for the analysis of radon potential based on environmental geology and geographically weighted regression. Environ. Model. Softw. 54, 165–181. https://doi.org/10.1016/j.envsoft.2014.01.006.
Pekel, J.F., Cottam, A., Gorelick, N., Belward, A.S., 2016. High-resolution mapping of global surface water and its long-term changes. Nature 540, 418–422. https://doi.org/10.1038/nature20584.
Poggio, L., De Sousa, L.M., Batjes, N.H., Heuvelink, G.B.M., Kempen, B., Ribeiro, E., Rossiter, D., 2021. SoilGrids 2.0: producing quality-assessed soil information for the globe. SOIL Discuss 7, 217–240. https://doi.org/10.5194/soil-7-217-2021.
Poorter, L., Bongers, F., Aide, T.M., Almeyda Zambrano, A.M., Balvanera, P., Becknell, J. M., Boukili, V., Brancalion, P.H.S., Broadbent, E.N., Chazdon, R.L., Craven, D., de Almeida-Cortez, J.S., Cabral, G.A.L., de Jong, B.H.J., Denslow, J.S., Dent, D.H., DeWalt, S.J., Dupuy, J.M., Durán, S.M., Rozendaal, D.M.A., 2016. Biomass resilience of Neotropical secondary forests. Nature 530 (7589), 211–214. https://doi.org/10.1038/nature16512.

Poorter, L., Craven, D., Jakovac, C.C., van der Sande, M.T., Amissah, L., Bongers, F., Chazdon, R.L., Farrior, C.E., Kambach, S., Meave, J.A., Muñoz, R., Norden, N., Rüger, N., van Breugel, M., Almeyda Zambrano, A.M., Amani, B., Andrade, J.L., Brancalion, P.H.S., Broadbent, E.N., de Foresta, H., Dent, D.H., Derroire, G., DeWalt, S.J., Dupuy, J.M., Durán, S.M., Fantini, A.C., Finegan, B., Hernández-Jaramillo, A., Hernández-Stefanoni, J.L., Hietz, P., Junqueira, A.B., N'dja, J.K., Letcher, S.G., Lohbeck, M., López-Camacho, R., Martínez-Ramos, M., Melo, F.P.L., Mora, F., Müller, S.C., N'Guessan, A.E., Oberleitner, F., Ortiz-Malavassi, E., Pérez-García, E.A., Pinho, B.X., Piotto, D., Powers, J.S., Rodríguez-Buriticá, S., Rozendaal, D.M.A., Ruíz, J., Tabarelli, M., Teixeira, H.M., de Sá, Valadares, Barretto Sampaio, E., van der Wal, H., Villa, P.M., Fernandes, G.W., Santos, B.A., Aguilar-Cano, J., de Almeida-Cortez, J.S., Alvarez-Davila, E., Arreola-Villa, F., Balvanera, P., Becknell, J.M., Cabral, G.A.L., Castellanos-Castro, C., de Jong, B.H.J., Nieto, J.E., Espírito-Santo, M.M., Fandino, M.C., García, H., García-Villalobos, D., Hall, J.S., Idárraga, A., Jiménez-Montoya, J., Kennard, D., Marín-Spiotta, E., Mesquita, R., Nunes, Y.R.F., Ochoa-Gaona, S., Peña-Claros, M., Pérez-Cárdenas, N., Rodríguez-Velázquez, J., Villanueva, L.S., Schwartz, N.B., Steininger, M.K., Veloso, M.D.M., Vester, H.F.M., Vieira, I.C.G., Williamson, G.B., Zanini, K., Hérault, B., 2021. Multidimensional tropical forest recovery. Science 374 (6573), 1370–1376. https://doi.org/10.1126/science.abh3629.

Pugh, T.A., Lindeskog, M., Smith, B., Poulter, B., Arneth, A., Haverd, V., Calle, L., 2019. Role of forest regrowth in global carbon sink dynamics. Proceedings of the National Academy of Sciences 116 (10), 4382–4387. https://doi.org/10.1073/pnas.1810512116.

Ratner, B., 2009. The correlation coefficient: Its values range between 1/1, or do they. J. Target. Meas. Anal. Mark. 17 (2), 139–142. https://doi.org/10.1057/jt.2009.5.

Requena Suarez, D., Rozendaal, D.M.A., De Sy, V., Gibbs, D.A., Harris, N.L., Sexton, J.O., Feng, M., Channan, S., Zahabu, E., Silayo, D.S., Pekkarinen, A., Martius, C., Herold, M., 2021. Variation in aboveground biomass in forests and woodlands in Tanzania along gradients in environmental conditions and human use. Environ. Res. Lett. 16 (4) https://doi.org/10.1088/1748-9326/abe960.

Requena Suarez, D., Rozendaal, D.M.A., De Sy, V., Decuyper, M., Málaga, N., Durán Montesinos, P., Arana Olivos, A., De la Cruz Paiva, R., Martius, C., Herold, M., 2023. Forest disturbance and recovery in Peruvian Amazonia. Glob. Chang. Biol. 00, 1–22. https://doi.org/10.1111/gcb.16695.

Ribeiro, M.C., Metzger, J.P., Martensen, A.C., Ponzoni, F.J., Hirota, M.M., 2009. The Brazilian Atlantic Forest: How much is left, and how is the remaining forest distributed? Implications for Conservation. Biological Conservation 142 (6), 1141–1153. https://doi.org/10.1016/j.biocon.2009.02.021.

Roderick, M.L., Farquhar, G.D., Berry, S.L., Noble, I.R., 2001. On the direct effect of clouds and atmospheric particles on the productivity and structure of vegetation. Oecologia 129 (1), 21–30. https://doi.org/10.1007/s004420100760.

Roesch, L.F.W., Vieira, F.C.B., Pereira, V.A., Schünemann, A.L., Teixeira, I.F., Senna, A.J. T., Stefenon, V.M., 2009. The Brazilian Pampa: A fragile biome. Diversity 1 (2), 182–198. https://doi.org/10.3390/d1020182.

Saatchi, S.S., Harris, N.L., Brown, S., Lefsky, M., Mitchard, E.T.A., Salas, W., Zutta, B.R., Buermann, W., Lewis, S.L., Hagen, S., Petrova, S., White, L., Silman, M., Morel, A., 2011. Benchmark map of forest carbon stocks in tropical regions across three continents. Proc. Natl. Acad. Sci. 108 (24), 9899–9904. https://doi.org/10.1073/pnas.1019576108.

Santoro, M., Cartus, O., Carvalhais, N., Rozendaal, D.M.A., Avitabile, V., Araza, A., de Bruin, S., Herold, M., Quegan, S., Rodríguez-Veiga, P., Balzter, H., Carreiras, J., Schepaschenko, D., Korets, M., Shimada, M., Itoh, T., Moreno Martínez, Á., Cavlovic, J., Gatti, R.C., Willcock, S., 2021. The global forest above-ground biomass pool for 2010 estimated from high-resolution satellite observations. Earth Syst. Sci. Data 13 (8), 3927–3950. https://doi.org/10.5194/essd-13-3927-2021.

Shimabukuro, Y.E., Arai, E., Duarte, V., Dutra, A.C., Cassol, H.L.G., Sano, E.E., Hoffmann, T.B., 2020. Discriminating Land Use and Land Cover Classes in Brazil Based on the Annual PROBA-V 100 m Time Series. IEEE J. Sel. Top. Appl. Earth Obs. Remote Sens. 13, 3409–3420. https://doi.org/10.1109/JSTARS.2020.2994893.

Silva Junior, C.H.L., Heinrich, V.H.A., Freire, A.T.G., Broggio, I.S., Rosan, T.M., Doblas, J., Anderson, L.O., Rousseau, G.X., Shimabukuro, Y.E., Silva, C.A., House, J. I., Aragão, L.E.O.C., 2020. Benchmark maps of 33 years of secondary forest age for Brazil. Sci. Data 7 (1). https://doi.org/10.1038/s41597-020-00600-4.

Silva Junior, C.H.L., Buna, A.T.M., Bezerra, D.S., Costa, O.S., Santos, A.L., Basson, L.O.D., Santos, A.L.S., Alvarado, S.T., Almeida, C.T., Freire, A.T.G., Rousseau, G.X., Celentano, D., Silva, F.B., Pinheiro, M.S.S., Amaral, S., Kampel, M., Vedovato, L.B., Anderson, L.O., Aragão, L.E.O.C., 2022. Forest Fragmentation and Fires in the Eastern Brazilian Amazon–Maranhão State, Brazil. Fire 5 (3). https://doi.org/10.3390/fire5030077.

Slik, J.W.F., Bernard, C.S., van Beek, M., Breman, F.C., Eichhorn, K.A.O., 2008. Tree diversity, composition, forest structure and aboveground biomass dynamics after single and repeated fire in a Bornean rain forest. Oecologia 158 (3), 579–588. https://doi.org/10.1007/s00442-008-1163-2.

Smith, C.C., Espírito-Santo, F.D.B., Healey, J.R., Young, P.J., Lennox, G.D., Ferreira, J., Barlow, J., 2020. Secondary forests offset less than 10% of deforestation-mediated carbon emissions in the Brazilian Amazon. Glob. Chang. Biol. 26 (12), 7006–7020. https://doi.org/10.1111/gcb.15352.

Souza, C.M., Shimbo, J.Z., Rosa, M.R., Parente, L.L., Alencar, A.A., Rudorff, B.F.T., Hasenack, H., Matsumoto, M., Ferreira, L.G., Souza-Filho, P.W.M., de Oliveira, S.W., Rocha, W.F., Fonseca, A.V., Marques, C.B., Diniz, C.G., Costa, D., Monteiro, D., Rosa, E.R., Vélez-Martin, E., Azevedo, T., 2020. Reconstructing three decades of land use and land cover changes in brazilian biomes with landsat archive and earth engine. Remote Sens. (Basel) 12 (17). https://doi.org/10.3390/RS12172735.

Sundqvist, M.K., Sanders, N.J., Wardle, D.A., 2013. Community and ecosystem responses to elevational gradients: Processes, mechanisms, and insights for global change. Annu. Rev. Ecol. Evol. Syst. 44 (November), 261–280. https://doi.org/10.1146/annurev-ecolsys-110512-135750.

Tian, F., Qiu, G.Y., Yang, Y.H., Xiong, Y.J., Wang, P., 2012. Studies on the relationships between land surface temperature and environmental factors in an inland river catchment based on geographically weighted regression and MODIS data. IEEE J. Selected Top. Appl. Earth Observ. Remote Sens. 5 (3), 687–698. https://doi.org/10.1109/JSTARS.2012.2190978.

Tobler, W.R., 1970. A computer movie simulating urban growth in the detroit region. Economic Geography 46.

Urbazaev, M., Thiel, C., Cremer, F., Dubayah, R., Migliavacca, M., Reichstein, M., Schmullius, C., 2018. Estimation of forest aboveground biomass and uncertainties by integration of field measurements, airborne LiDAR, and SAR and optical satellite data in Mexico. Carbon Balance Management 13 (1). https://doi.org/10.1186/s13021-018-0093-5.

Wang, J.-F., Liu, X., Christakos, G., Liao, Y.-L., Gu, X., & Zheng, X.-Y. (2010). Assessing local determinants of neural tube defects in the Heshun Region, Shanxi Province, China. http://www.biomedcentral.com/1471-2458/10/52.

Wang, Q., Ni, J., Tenhunen, J., 2005. application of a geographically-weighted regression analysis to estimate net primary production of Chinese Forest Ecosystems. Source Global Ecol. Biogeogr. 14 (4), 379–393. https://doi.org/10.1111/j.1466-8.

Wang, C., Zhang, J., Yan, X., 2012. The use of geographically weighted regression for the relationship among extreme climate indices in China. Math. Probl. Eng. 2012 https://doi.org/10.1155/2012/369539.

White, J.C., Hermosilla, T., Wulder, M.A., Coops, N.C., 2022. Mapping, validating, and interpreting spatio-temporal trends in post-disturbance forest recovery. Remote Sens. Environ. 271 https://doi.org/10.1016/j.rse.2022.112904.

Xu, G., Wang, W., Lu, D., Lu, B., Qin, K., Jiao, L., 2022. Geographically varying relationships between population flows from Wuhan and COVID-19 cases in Chinese cities. Geo-Spatial Inform. Sci. 25 (2), 121–131. https://doi.org/10.1080/10095020.2021.1977093.

Zarin, D.J., Davidson, E.A., Brondizio, E., Vieira, I.C.G., Sa, T., Feldpausch, T., Schuur, E. A.G., Mesquita, R., Moran, E., Delamonica, P., Ducey, M.J., Hurtt, G.C., Salimon, C., Denich, M., 2005. Legacy of Fire Slows Carbon Accumulation in Amazonian Forest Regrowth. Front. Ecol. Environ. 3 (7), 365. https://doi.org/10.2307/3868585.